



HAL
open science

Streamless aggregation of in the presence of isopropylidenadenosin

Christiane Hilgardt, Jitka Cejkova, Marcus J.B. Hauser, Hana Sevcíkova

► **To cite this version:**

Christiane Hilgardt, Jitka Cejkova, Marcus J.B. Hauser, Hana Sevcíkova. Streamless aggregation of in the presence of isopropylidenadenosin. *Biophysical Chemistry*, 2007, 132 (1), pp.9. 10.1016/j.bpc.2007.09.013 . hal-00501684

HAL Id: hal-00501684

<https://hal.science/hal-00501684>

Submitted on 12 Jul 2010

HAL is a multi-disciplinary open access archive for the deposit and dissemination of scientific research documents, whether they are published or not. The documents may come from teaching and research institutions in France or abroad, or from public or private research centers.

L'archive ouverte pluridisciplinaire **HAL**, est destinée au dépôt et à la diffusion de documents scientifiques de niveau recherche, publiés ou non, émanant des établissements d'enseignement et de recherche français ou étrangers, des laboratoires publics ou privés.

Accepted Manuscript

Streamless aggregation of *Dictyostelium* in the presence of isopropylidenadenosin

Christiane Hilgardt, Jitka Cejkova, Marcus J.B. Hauser, Hana Sevcíkova

PII: S0301-4622(07)00234-7
DOI: doi: [10.1016/j.bpc.2007.09.013](https://doi.org/10.1016/j.bpc.2007.09.013)
Reference: BIOCHE 5025

To appear in: *Biophysical Chemistry*

Received date: 4 September 2007
Accepted date: 27 September 2007



Please cite this article as: Christiane Hilgardt, Jitka Cejkova, Marcus J.B. Hauser, Hana Sevcíkova, Streamless aggregation of *Dictyostelium* in the presence of isopropylidenadenosin, *Biophysical Chemistry* (2007), doi: [10.1016/j.bpc.2007.09.013](https://doi.org/10.1016/j.bpc.2007.09.013)

This is a PDF file of an unedited manuscript that has been accepted for publication. As a service to our customers we are providing this early version of the manuscript. The manuscript will undergo copyediting, typesetting, and review of the resulting proof before it is published in its final form. Please note that during the production process errors may be discovered which could affect the content, and all legal disclaimers that apply to the journal pertain.

Streamless aggregation of *Dictyostelium* in the presence of isopropylidenadenosin

Christiane Hilgardt, Jitka Čejková, Marcus J.B. Hauser, Hana Ševčíková

corresponding author: Christiane Hilgardt

postal address: Otto-von-Guericke-University Magdeburg, Institute of Experimental Physics, Biophysics Group, Universitätsplatz 2, 39106 Magdeburg, Germany

fax: ++49 (0)391 67 11181

telephone: ++49 (0)391 67 18334

e-mail address: christiane.hilgardt@physik.uni-magdeburg.de

number of pages: 20

number of tables: 0

illustrations: 8

Streamless aggregation of *Dictyostelium* in the presence of isopropylidenadenosin

Christiane Hilgardt ^{a,*}, Jitka Čejková ^b, Marcus J.B. Hauser ^a, Hana Ševčíková ^b

^a *Otto-von-Guericke-University Magdeburg, Institute of Experimental Physics, Biophysics Group, Universitätsplatz 2, 39106 Magdeburg, Germany*

^b *Center for Nonlinear Dynamics of Chemical and Biological Systems, Institute of Chemical Technology, Prague, Technická 5, 166 28 Prague 6, Czech Republic*

* *corresponding author*

e-mail: christiane.hilgardt@physik.uni-magdeburg.de

Abstract

Starving cells of *Dictyostelium discoideum* undergo a developmental cycle where cAMP is autocatalytically produced and relayed from cell to cell, resulting in the propagation of excitation waves over a spatially extended population. Later the homogeneous cell layer transforms into a pattern of cell streams directed perpendicular to the cAMP waves. Here we chemically influence aggregation competent cells by isopropylidenadenosin (IPA), an adenosine derivative. It can be assumed, that IPA acts via specific adenosine binding sites localized in the cellular membrane. We find, however, that pattern formation and cellular aggregation under the influence of IPA differ considerably compared to experiments with adenosine. In particular, our observations point towards an inhibitory effect on adenylate cyclase (ACA), the key enzyme in the autocatalytic production process of cAMP inside the cell. Our results suggest the existence of a direct coupling (via intracellular affection) or indirect coupling (via inhibition of cAMP binding) of the specific adenosine receptors to the regulatory circuit that controls cyclic intra- and extracellular cAMP concentration.

Keywords: signal transduction, adenosine derivative, chemical inhibition, ACA activity, excitability, abnormal chemotaxis

1 Introduction

Amoeboid cells of *Dictyostelium discoideum* live in soil as autonomous single cells. Upon nutrient deprivation they undergo a complex developmental cycle which includes the transition from uni- to multicellular organization through a succession of morphological states. Aggregation is the first process to occur during the morphogenetic development of a starving population into fruiting bodies. The aggregation is mediated by the relay of adenosine-3',5'-cyclic monophosphate (cAMP) that acts as a positive chemoattractant ensuring the coordinated aggregation of the cells [1; 2].

At the onset of the developmental cycle, individual cells synthesize cAMP autonomously and secrete it into their environment. At neighbouring cells, the signal is detected via highly specific surface

receptors [3; 4; 5], inducing various signal transduction cascades within the cells. Through the activation of membrane-bound adenylate cyclase (ACA) one of them leads to autocatalytic synthesis of cAMP and its secretion into the cellular environment [6; 7]. Binding of extracellular cAMP to the membrane receptors also triggers the production of cGMP that is involved in the chemotactic cell movement [8; 9; 10; 11; 12].

The excitation process is followed by a refractory period, where receptor phosphorylation and inactivation of ACA is involved, before the cells become deadapted and excitable again. During the refractory period the extracellular cAMP concentration is decreased by the external and membrane-bound phosphodiesterase (PDE), which is regulated by the phosphodiesterase inhibitor (PDI) [13; 14; 15].

These processes are manifested in the generation of aggregation centres, which periodically emit outwardly moving concentration waves of cAMP [16; 17; 6]. The waves propagate as concentric waves (target waves) or spiral waves due to wave interaction. The cells move chemotactically against the emitted waves, organize in characteristic streaming patterns and, at later stages of aggregation, accumulate in the aggregation centers. After passing through a mound and a motile slug stages, the aggregates transform into fully differentiated fruiting bodies, containing germinable spores.

In the present paper we report on the effects exerted by isopropyladenosin (IPA) in the course of pattern formation and cell aggregation in *D. discoideum*. IPA belongs to the group of adenosine derivatives that have been shown to affect binding of cAMP to the cAMP-specific surface receptors [18]. However, we have found that the course of aggregation in the presence of IPA differs considerably from that observed in the presence of adenosine [19]. Although the cells on IPA agar relay the cAMP signal, and optical density waves can be observed in dark-field as in the case of adenosine [19], the cells do never form any characteristic streaming patterns due to a concerted cell movement. Instead, the waves vanish after a certain time leaving the cell layer in a homogeneous state. Later, many aggregation centres emerge simultaneously all over the petri dish. These centres attract cells from their closest neighbourhood, however, again without visible stream formation. The aggregates then undergo morphogenesis leading to the formation of normally proportioned fruiting bodies.

2 Experimental

Growth conditions and initiation of starvation

Cells of the *D. discoideum* strain AX2 were cultured from frozen spores in axenic HL5-medium at 21°C [20] and harvested in the second half of the exponential growth phase. To remove all nutrients from the environment and thus to initiate starvation the cells were washed twice in phosphate buffer (16 mM KH_2PO_4 , Na_2HPO_4 , pH 6.14) and pelletized by low speed centrifugation. After re-suspension in phosphate buffer the cells were spread homogeneously onto agar plates (0.5 % Difco Bacto-Agar in phosphate buffer, 2 mM caffeine) at a density of 6.2×10^5 cells/cm². IPA was dissolved in the buffer used to prepare the agar plates. After removal of the supernatant, the plates were incubated at 21°C in darkness for 4 to 5 h until the first excitation waves appeared.

Chemotactic assays

Single drops ($0.5 \mu\text{l}$) of nutrient-free cell suspension (2×10^7 cells/ml) were placed at a distance of a few millimetres around droplets ($0.5 \mu\text{l}$) containing cAMP (2.5×10^{-8} M) on agar plates with either 0.25 mM IPA or IPA-free control plates. After a few hours the displacement of cells was evaluated. Similarly, the chemotactic response to IPA gradients was examined.

Yield of spores

Washed cells were allowed to complete their developmental cycle on agar plates (2% Bacto-agar in phosphate buffer) with 0, 0.25, 0.5 and 1 mM IPA. The total number of developed spores out of a known number of vital cells was determined by microscopic observation.

Visualization techniques

The propagation of cAMP waves can be observed indirectly in dark-field [16; 2]), where optical density waves are caused by changes in cell shape and coherent cell movement depending on the excitation state of the cells. The optics of our dark-field set-up follows that of [17]. Images were taken at intervals of 3 s with a CCD camera (Hamamatsu C3077), digitized (DT-Open Layers DT 3155 Mach Series Frame Grabber), and stored as 8-bit images on hard disc. The behaviour of single cells within a population was observed with an inverse microscope (Zeiss Axiovert 200) equipped with a $10\times$ PlanNeoFluar objective and a CCD camera (Hamamatsu C2400-07). Images were sampled at 1 min intervals.

Data analysis

To evaluate the temporal development of the wave parameters, space-time plots were constructed from the sequences of grabbed images according to the method described by [21]. Changes in wave shape were visualized by extracting the grey values of one point in space along the time axis of the space-time plots. These profiles were normalized, and smoothed by moving average. Global trends were removed by polynomial regression. The standard deviation of all normalized data in a time series was taken as a measure of the wave amplitude. Power spectra were constructed by Fast Fourier Transformation of time series at single points in space.

3 Results

The effect of IPA on pattern formation was first studied in dark-field. Figure 1 shows snapshots obtained in the presence of IPA and under control conditions, respectively. Under both conditions excitation waves can be observed about 5 h after the initiation of starvation. However, the early waves in the presence of IPA can hardly be seen in dark-field, and their visualization requires further image processing in order to recover the appearance of the first low-amplitude waves originating at different random positions (Fig. 1(a)). During the following 2 h these patterns develop into stable,

well visible spiral waves (Fig. 1(b)-(c)). One of the most remarkable differences to the experiment under control conditions is the formation of huge spirals, whose diameters may attain a few centimetres (Fig. 1(d)). Indeed, in the IPA concentration range between 0.125 to 2 mM spirals with diameters greater than 4 cm can be observed. Their extension is typically limited by the borders of the petri dish. By contrast, the diameter of a spiral domain in control experiments is typically a few millimetres (Fig. 1(a)).

While the control cells have already reached the state of late aggregation with tight cell-cell contacts and stream formation, the cells on IPA-containing agar still form a homogeneous layer (Fig. 1(e)). A continuous change in homogeneity caused by directed cell movement towards the spiral centres leading to stream formation is not observed even after 10.5 h of starvation (Fig. 1(f)). This is also reflected in the faint territory borders where colliding cAMP-waves annihilate. Although the waves propagate as undisturbed, smooth fronts for at least 2 h the spirals suddenly and simultaneously disappear throughout the petri dish. Within each territory, this happens from inside to outside, i.e. spiral rotation around a core suddenly stops and the inner open end of the spiral propagates to the border of the petri dish where it is annihilated (Fig. 1(e)). During the following transition phase, which can last for up to 2 h, the cell layer seems to be inactive. However, image processing reveals the occurrence of concentric waves with large wave lengths at seemingly random positions in the yet homogeneous cell layer (Fig. 1(f)). Suddenly, many small oscillatory regions emerge, emitting short-range target waves that attract the cells in their closest neighbourhood. These waves cause a break-up of the cell layer into many miniature territories (Fig. 1(g)-(h)). Again, no visible stream-like structures evolve. Later, these clusters transform into mounds (Fig. 1(h)). After approx. 30 h the developmental cycle is complete. Many small, but normally proportioned fruiting bodies develop.

Occasionally it can be observed that after mound formation individual mounds connect by tube-like, more or less unbranched structures (Fig. 2). Within these "streams" adjacent mounds are absorbed by the attracting mounds. Further analysis shows that these mounds elicit high-frequency target waves inducing cell migration over distances up to 3 mm. In contrast to the observations in the wild type strain DH1 [22; 5] these mounds do not have ring-like forms, although the inverted representation of these structures in Figure 2 lead to that optical impression. Furthermore, these mounds do not break or change their position.

To extract the basic parameters of wave propagation, space-time plots were constructed. Figure 3(a) and (b) correspond to wave patterns observed within one experiment, where patterns in (a) evolved on control agar and (b) on agar containing 0.25 mM IPA.

The evolution of wave propagation within the two cell layers can be followed directly along the time axis, as well as the respective temporal changes in cell density (i.e. in the homogeneity of the medium). While in Figure 3(a) chemotactic cell aggregation progresses continuously, yielding distinct, separated aggregation territories, in 3(b) wave initiation suddenly ceases. The homogeneity of the cell layer does not show any pronounced changes with time caused by directed cell movement towards the centres. Merely the core of the spiral shown in Figure 3(b) increases during the last three propagating waves. The extension of the spiral domain exceeds the area of the spatial axis,

whereas under control conditions several individual spiral centres evolve at the same spatial scale. Figure 3(c) was constructed from sections through the right images of Figure 1. It covers a time interval of more than 9 h summarizing the different developmental states in the presence of IPA (early patterns with huge spirals (I), disappearance of spiral waves and transition phase (II), secondary patterns with small clusters emitting target waves (III)).

Typical wave profiles obtained from grey values at given fixed positions in space plotted as function of time are shown in Figure 4. High values correspond to the bright bands of the original wave pattern and are caused by prolonged cell shapes due to the excitation process and chemotactic movement. In general, wave profiles can give information about the coherence of a cell population in their chemotactic response. Figure 4(a) was constructed from Figure 3(a), which was obtained under control conditions. These waves show regular oscillations with a tendency to biphasic behaviour, as seen from the presence of a small secondary peak within one period. The corresponding power spectra consist of two harmonic frequencies with a periodicity of 5 and 2.5 min, respectively. The shape of individual waves during advanced spiral propagation in the presence of 0.25 mM IPA (corresponding to the time-frame shown in Figure 1 (c)-(d), right-hand side) is shown in Figure 4(b). These waves possess a plateau-like form at high grey values indicating the pronounced cellular response to passing waves. Power spectra reveal several frequencies with a periodicity between 1.4 to 6.0 min. The amplitudes of the waves were not affected by the presence of IPA (0.125 - 2 mM) in the agar. Secondary target waves emitted after mound formation (Figure 1(g)-(h), right-hand side) lead to very regular oscillations for approx. 1.5 h with a periodicity of about 7.5 min (Fig. 4(c)).

The change in the rotation period of successive waves under control conditions and in the presence of IPA is shown in Figure 5(a). The values for the experiments with IPA have been obtained from fully developed spiral waves occurring in early wave patterns (developmental state in Figure 1(c)-(e), right-hand side). The change in period of successive waves does not show any significant concentration dependency. Even 0.125 mM IPA causes initially long periods. With each propagating wave the period shortens and eventually reaches values around 6.5 min. After a phase of stagnation the period increases again to values close to the initial values before the waves die out (according to Figure 1(e), right-hand side). Approximately 25 rotations can be observed on IPA-containing agar before wave cessation in a still homogeneous cell layer. In control experiments periods of rotating spiral waves stay roughly constant at values ~ 5 min for the first 20 rotations, before the period begins to shorten. In this case, up to 39 rotations could be analyzed before the waves become invisible in dark-field due to tight cell-cell contacts. In contrast, the propagation velocity of waves on IPA-containing agar - represented by the slopes of each wave band in the space-time plots (Fig. 3) - do not differ significantly from those obtained under control conditions, neither in magnitudes nor in their temporal evolution (Fig. 5(b)). For any condition the velocity of successive waves decreases continuously from ~ 0.4 mm/min to 0.25 mm/min.

Figure 6 shows the propagation velocity of subsequent wave fronts as a function of the rotation period, i.e. the time required for a full rotation of the spiral wave. Under control conditions the dispersion relation follows the general course known from other excitable media, i.e. the velocity decreases with decreasing period [21]. In the presence of IPA the form of the dispersion relation is

more complex. For the first few waves the curve follows the common trend (their propagation velocities decrease with the period) even though this occurs in a range of larger periods and with less steep course. In a transitory domain, the period remains more or less constant while the velocity still decreases. Before the waves vanish the period increases once more while the propagation velocity decreases, resulting in a "backward" turn of the dispersion curve.

To investigate both the capability of starving cells to sense a cAMP gradient and the chemotactic response in the presence of IPA, chemotactic assays were prepared. It was found, that cells incubated on IPA-containing agar are basically able to sense cAMP and move up a gradient. In contrast, IPA exerts no chemotactic attraction on the cells.

To specify the effect of IPA, the cells were allowed to starve under standard conditions until spiral waves were fully developed. Then a fine mist of IPA in phosphate buffer (2 mM) was sprayed homogeneously onto the cell layer. Experiments were conducted with varying IPA concentrations. No immediate effect of IPA on spiral wave patterns was observed. The appearance of spiral waves was not disturbed and the sizes of the areas occupied by individual spirals did not change. Although growth of territory borders was observed, in most cases no streams were formed. As in the case of cells incubated on agar containing IPA, the spiral waves disappeared after some time, the primordial borders became washed out, and corresponding territories disintegrated into subsystems of many small cell clusters.

Phase contrast microscopic investigations of the behaviour of cells within a population confirms the absence of streaming patterns and the lack of obvious morphological correlation between the first spiral waves and the resulting distribution of fruiting bodies. Figure 7 shows a time series of experimental results in the presence of 1 mM IPA. Image recording was started immediately after cell preparation. After 5 to 6 h a continuous increase in local cell density can be observed (Fig. 7(b)). Parallel investigations in dark-field reveal that this developmental state approximates the phase of early spiral propagation. Even when the cells start to assemble, neither local clustering nor stream formation can be observed. Furthermore, cell prolongation, i.e. indication of cellular polarization processes in response to cAMP waves, sets in after 8.9 h. 11 h after initiation of starvation, the cells are attracted by areas of particularly high cell density (Fig. 7(c)), upper left corner and darker areas in Figure 7(d), indicated by arrows). Periodic cell movement towards these centres as well as cell prolongation can now clearly be observed. This period can be associated to the state of aggregation corresponding to Figure 7(g). However, individual cells seem to respond to more than one high density centre and change their direction frequently. In Figure 7(e) a distinct aggregation centre has been established in the upper part of the image, which at a later stage forms a mound (Fig. 7(f)). Elsewhere smaller centres have dissolved. The mound reshapes many times and never forms a compact cell aggregate (Fig. 7(g)-(j)). Several thin, long fingers protrude as multiple tips. Fusion and reforming of the fingers repeats for a long time. Thicker fingers appear and separate from the aggregate (Fig. 7(i)-(k)). These motile slugs disrupt frequently into smaller slugs, which sometimes regress into mounds before converting into slugs again (Fig. 7(l)-(n)). Approximately 30 h after the initiation of starvation normally proportioned fruiting bodies were formed from slugs typically without any previous culmination phase (Fig. 7(o)). Surprisingly, the yield of spores from

fruiting bodies developed on agar containing IPA is significantly about 2.5 times higher than under standard conditions (Fig. 9).

4 Discussion

Excitability of *D. discoideum* cells during the developmental cycle is mainly determined by their sensitivity to cAMP, depending on the amount and affinity of receptors, and by the level of cAMP output, based on ACA activity [23]. Thus, it was shown, that an overall decrease in excitability by changing the affinity to extracellular cAMP [5] (e.g. via modification of the receptor composition) or by external chemical influence [24; 21; 25] (e.g. via the addition of caffeine, resulting in an inhibition of the cAMP-dependent activation of the ACA and in altered chemotactic adaptation) can lead to a wave length increase and, at the same time to a dramatic enlargement of the aggregation territories and an inhibition of centre initiation.

In the present paper we examined the influence of IPA, an adenosine derivative, on cAMP pattern formation and on the developmental cycle. Adenosine is a physiological degradation product of cAMP and has been shown to inhibit several cAMP-depending processes by inhibition of cAMP binding [19] and postaggregative differentiation [18]. Adenosine reduces oscillatory cAMP activity [26; 19; 27] and plays a role in cell type regulation at later states of the developmental cycle [28; 29]. In spite of the structural similarity, adenosine does not compete with cAMP for the cAMP surface receptors [26; 19]. Instead, adenosine acts non-competitively and indirectly through β -receptors as one of the cellular adenosine binding sites [26; 30; 18]. Alterations in the ribose moiety of adenosine in most cases increases the inhibitory effect on cAMP binding [18].

It has been shown that IPA as an adenosine derivative decreases the cAMP binding to the cAMP surface receptors dramatically [18]. Here we show, that similarly to the effect of adenosine, IPA has an inhibitory action on the initiation of aggregation centre formation, leading to oversized spiral wave domains (Fig. 1). In addition, the appearance of coherent spiral patterns is delayed, though IPA does not prevent signal release. Although one can assume that the effect of IPA is mediated by binding to the adenosine specific surface receptors, our results on the effect of IPA on developmental processes differ clearly from the results obtained from experiments with adenosine [19]. Moreover, our observations point towards a strong inhibitory effect of IPA on ACA, the key enzyme of cAMP production, which couples to the regulatory circuit that controls cyclic increases of intra- and extracellular cAMP [31; 23; 32]. In general, the inhibition of ACA results in a decrease in excitability of the system influencing in turn the extension and distribution of aggregation territories.

In the presence of IPA no visible stream-like structures evolve during the whole developmental cycle (Fig. 1, 3, 7). Streamless aggregation in *D. discoideum* has also been observed in null mutants of *acaA* which encodes ACA [33]. It has been shown that *acaA*⁻ cells have polarity defects and fail to aggregate in stream-like structures. Stream formation results from a head to tail arrangement of the cells, which is regulated by the asymmetric ACA localization at the uropod of the cells [33].

ACA-deficient cells are able to polarize and move up a cAMP gradient when stimulated, but are unable to form streams. In the presence of IPA we have observed a long-lasting homogeneity of the

cell layer, which later transforms into streamless accumulation of cells at the aggregation centres. Microscopical observations confirm that this impression results from directed cell movement proceeding without head to tail arrangement, which results in a local cell density increase around the attracting aggregation centres (Fig. 7). Moreover, the ACA independent polarization process of the cells, induced by external cAMP, and required for the chemotactic cell movement, is delayed (Fig. 7). In [32] it has been shown that *acaA⁻* cells are able to orient in spatial and temporal cAMP-gradients, but exhibit chemotactic defects. In particular, these cells show a reduced suppression of lateral pseudopod formation and cell turning, resulting in highly inefficient chemotaxis and randomly appearing effective direction.

A close correlation exists between the frequency of spiral rotation and the formation of stable signaling centres in *D. discoideum* [5]. Mutants in cAMP receptors that show low frequency of wave initiation and wave length, respectively, have difficulties in forming stable aggregation territories, because stable centre formation seems to require an equilibrium between the period of cAMP waves, chemotactic response and cell dispersion due to random cell movement [5]. In the case of IPA the potential role of random cell movement is suggested by the delayed and faintly developing territory borders, which reveal undirected cell movement. It appears that IPA forces the cells into a parameter regime, where the effect of random cell movement between successive waves does no longer allow the formation of stable aggregation centres.

Acknowledgements

C.H. is indebted to C.J. Weijer for the information about IPA. C.H. was supported by the Deutsche Forschungsgemeinschaft (grant MU 884/18-2). J.C. and H.S. acknowledge the financial support of Ministry of Education of the Czech Republic (Research project MSM 6046137306) and of the Grant Agency of the Czech Republic (grants 204/04/1421 and 104/03/H141).

References

- [1] W. Roos, V. Nanjundiah, D. Malchow, and G. Gerisch, Amplification of cyclic-AMP signals in aggregating cells of *Dictyostelium discoideum*, FEBS Lett. 53 (1975) 139-142.
- [2] K.J. Tomchik and P.N. Devreotes, Adenosine 3',5'-monophosphate waves in *Dictyostelium discoideum*: a demonstration by isotope dilution-fluorography, Science 212 (1981) 443-446.
- [3] D. Malchow and G. Gerisch, Cyclic AMP binding to living cells of *Dictyostelium discoideum* in presence of excess cyclic GMP, Biochem. Biophys. Res. Commun. 55 (1973) 200-204.

- [4] P.J. Van Haastert and R.J. De Wit, Demonstration of receptor heterogeneity and affinity modulation by nonequilibrium binding experiments. The cell surface cAMP receptor of *Dictyostelium discoideum*, J. Biol. Chem. 259 (1984) 13321-13328.
- [5] D. Dormann, J.Y. Kim, P.N. Devreotes and C.J. Weijer, cAMP receptor affinity controls wave dynamics, geometry and morphogenesis in *Dictyostelium*, J. Cell Sci. 114 (2001) 2513-2523.
- [6] M.C. Dinauer, S.A. MacKay and P.N. Devreotes, Cyclic 3',5'-AMP relay in *Dictyostelium discoideum* III. The relationship of cAMP synthesis and secretion during the cAMP signaling response, J. Cell Biol. 86 (1980) 537-544.
- [7] A. Theibert and P.N. Devreotes, Surface receptor-mediated activation of adenylate cyclase in *Dictyostelium*. Regulation by guanine nucleotides in wild-type cells and aggregation deficient mutants, J. Biol. Chem. 261 (1986) 15121-15125.
- [8] B. Wurster, K. Schubiger, U. Wick and G. Gerisch, Cyclic GMP in *Dictyostelium discoideum*, Oscillations and pulses in response to folic acid and cyclic AMP signals, FEBS Lett. 76 (1977) 141-144.
- [9] J.M. Mato, ATP increases chemoattractant induced cyclic GMP accumulation in *Dictyostelium discoideum*, Biochim. Biophys. Acta 540 (1978) 408-411.
- [10] F. Ross and P. Newell, Streamers: chemotactic mutants of *Dictyostelium discoideum* with altered cyclic GMP metabolism, Gen. Microbiol. 127 (1981).
- [11] G. Liu and P.C. Newell, Evidence that cyclic GMP regulates myosin interaction with the cytoskeleton during chemotaxis of *Dictyostelium*, J. Cell Sci. 90 (1988) 123-129.
- [12] G. Gerisch, Chemotaxis in *Dictyostelium*. Annu. Rev. Physiol. 44 (1982) 535-552.
- [13] Y.Y. Chang, Cyclic 3',5'-adenosine monophosphate phosphodiesterase produced by the slime mold *Dictyostelium discoideum*, Science 161 (1968) 57-59.
- [14] J.T. Bonner, E.M. Hall, S. Noller, F.B. Jr. Oleson and A.B. Roberts, Synthesis of cyclic AMP and phosphodiesterase in various species of cellular slime molds and its bearing on chemotaxis and differentiation, Dev. Biol. 29 (1972) 402-409.
- [15] R. Sucgang, C.J. Weijer, F. Siegert, J. Franke and R.H. Kessin, Null mutations of the *Dictyostelium* cyclic nucleotide phosphodiesterase gene block chemotactic cell movement in developing aggregates, Dev. Biol. 192 (1997) 181-192.
- [16] F. Alcantara and M. Monk, Signal propagation during aggregation in the slime mould *Dictyostelium discoideum*, J. Gen. Microbiol. 85 (1974) 321-334.
- [17] J.D. Gross, M.J. Peacey and D.J. Trevan, Signal emission and signal propagation during early aggregation in *Dictyostelium discoideum*, J. Cell Sci. 22 (1976) 645-656.

- [18] M.M. Van Lookeren Campagne, P. Schaap and P.J. van Haastert, Specificity of adenosine inhibition of cAMP-induced responses in *Dictyostelium* resembles that of the P site of higher organisms, *Dev. Biol.* 117 (1986) 245-251.
- [19] P.C. Newell and F.M. Ross, Inhibition by adenosine of aggregation centre initiation and cyclic AMP binding in *Dictyostelium*, *J. Gen. Microbiol.* (1982). 128:2715-2724.
- [20] M. Sussmann, in: *Methods in Cell Biology. Dictyostelium discoideum: Molecular Approaches to Cell Biology*, ed. J.A. Spudich, Cultivation and synchronous morphogenesis of *Dictyostelium* under controlled experimental conditions, vol. 28 (Academic Press, New York, 1987) p. 9
- [21] F. Siegert and C.J. Weijer, Digital image processing of optical density wave propagation in *Dictyostelium discoideum* and analysis of the effects of caffeine and ammonia, *J. Cell Sci.* 93 (1989) 325-335.
- [22] D. Dormann, B. Vasiev and C.J. Weijer, Propagating waves control *Dictyostelium discoideum* morphogenesis, *Biophys. Chem.* 72 (1998) 21-35.
- [23] S. Sawai, P.A. Thomason, E.C. Cox, An autoregulatory circuit for long-range self-organization in *Dictyostelium* cell populations, *Nature* 433 (2005) 323-326.
- [24] M. Brenner and S.D. Thoms, Caffeine blocks activation of cyclic AMP synthesis in *Dictyostelium discoideum*, *Dev. Biol.* 101 (1984) 136-146.
- [25] F. Siegert and C.J. Weijer, Analysis of optical density wave propagation and cell movement in the cellular slime mould *Dictyostelium discoideum*, *Physica D* 49 (1991) 224-232.
- [26] P.C. Newell, Cell surface binding of adenosine to *Dictyostelium* and inhibition of pulsatile signalling, *FEMS Microbiol. Lett.* 13 (1982) 417-421.
- [27] A. Theibert and P.N. Devreotes, Adenosine and its derivatives inhibit the cAMP signaling response in *Dictyostelium discoideum*, *Dev. Biol.* 106 (1984) 166-173.
- [28] C.J. Weijer and A.J. Durston, Influence of cyclic AMP and hydrolysis products on cell type regulation in *Dictyostelium discoideum*, *J. Embryol. Exp. Morphol.* 86 (1985) 19-37.
- [29] P. Schaap and M. Wang, Interactions between adenosine and oscillatory cAMP signaling regulate size and pattern in *Dictyostelium*, *Cell* 45 (1986) 137-144.
- [30] P.J. Van Haastert, Binding of cAMP and adenosine derivatives to *Dictyostelium discoideum* cells. Relationships of binding, chemotactic, and antagonistic activities, *J. Biol. Chem.* 258 (1983) 9643-9648.

- [31] M. Maeda, S. Lu, G. Shaulsky, Y. Miyazaki, H. Kuwayama, Y. Tanaka, A. Kuspa and W.F. Loomis, Periodic signaling controlled by an oscillatory circuit that includes protein kinases ERK2 and PKA, *Science* 304 (2004) 875-878.
- [32] V. Stepanovic, D. Wessels, K. Daniels, W.F. Loomis and D.R. Soll, Intracellular role of adenylyl cyclase in regulation of lateral pseudopod formation during *Dictyostelium* chemotaxis. *Eukaryot. Cell* 4 (2005) 775-786.
- [33] P.W. Kriebel, V.A. Barr and C.A. Parent, Adenylyl cyclase localization regulates streaming during chemotaxis, *Cell* 112 (2003) 549-560.

Figure captions

Figure 1

Effect of IPA on the course of aggregation as observed in dark-field. The left half of each image corresponds to control conditions, the right half to 0.25 mM IPA in agar. Both patterns appeared inside the same petri dish divided into two chambers. If indicated by an asterisk the visibility of wave patterns was enhanced by image subtraction of two successive images. Times corresponds to the time after the initiation of starvation.

Figure 2

Fusion of mounds observed on agar with 0.25 mM IPA (reversed representation). Mounds connect by thick cell "streams". The development from (a) to (d) required 8.5 hours.

Figure 3

Space-time plots corresponding to control conditions (a) and 0.25 mM IPA in agar (b) and (c). The patterns of (a) and (b) were observed within one petri dish, divided into two chambers. Arrows indicate the spiral core (1) and the open wave ends when wave initiation ceases (2). (c) originates from the right-hand side of the images in Figure 1. The positions of the sub-images (c)-(h) of Figure 3 on the time axis are indicated. Particular developmental steps in the presence of IPA are indicated in (c): early spiral waves (I), disappearance of spiral waves and transition phase (II), secondary wave patterning period (III).

Figure 4

Profiles of dark-field waves under control conditions (a), and with 0.25 mM IPA in agar (b) and (c). Early wave propagation is represented by (b), whereas the waves corresponding to (c) appeared 7.8 h later during mound formation.

Figure 5

Rotation period (a) and propagation velocity (b) in the presence of IPA. Between 3 and 8 spiral waves were analyzed for each IPA concentration. Arithmetic mean values were formed and slightly smoothed by moving averaging over time.

Figure 6

Dispersion relation based on the data of Figure 5. The time course is indicated by arrows.

Figure 7

Developmental cycle in the presence of 1 mM IPA observed by phase contrast microscopy over a time interval of 30 h. The exact times correspond to the duration after starvation has been initiated. (a) homogeneous cell layer before cell migration, (b)-(e) cell movement without stream formation, (f)-(j) mound state, development of multiple tips, (k)-(m) slug state, disruption into smaller

structures, (n)-(o) formation of fruiting bodies.

Figure 8

Yield of spores in dependence of the IPA concentration in agar with error bars as standard deviation. The initial cell density was 6.2×10^5 cells/cm². The values correspond to the percentage of the initial number of cells which transformed into spores.

ACCEPTED MANUSCRIPT

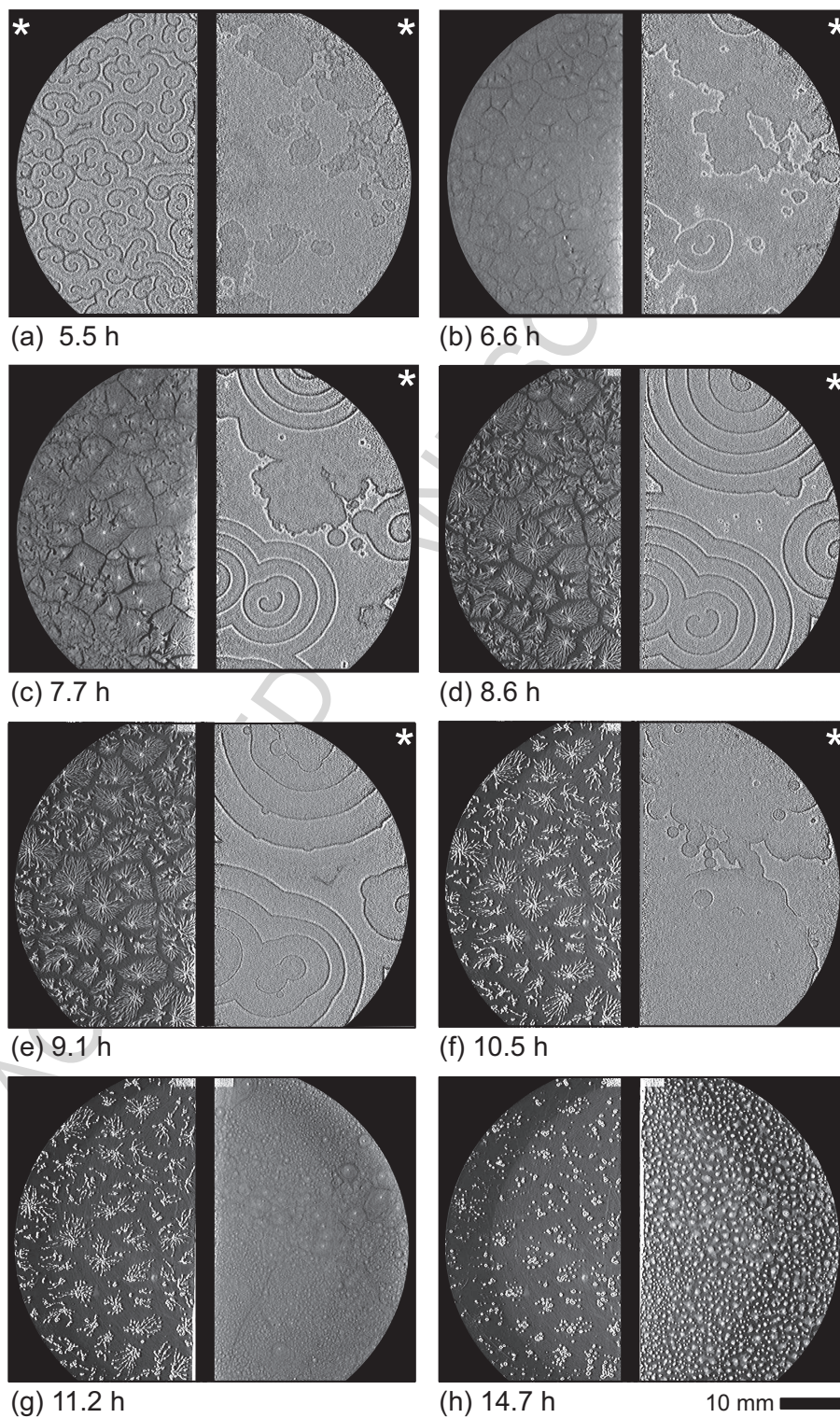


Figure 1:

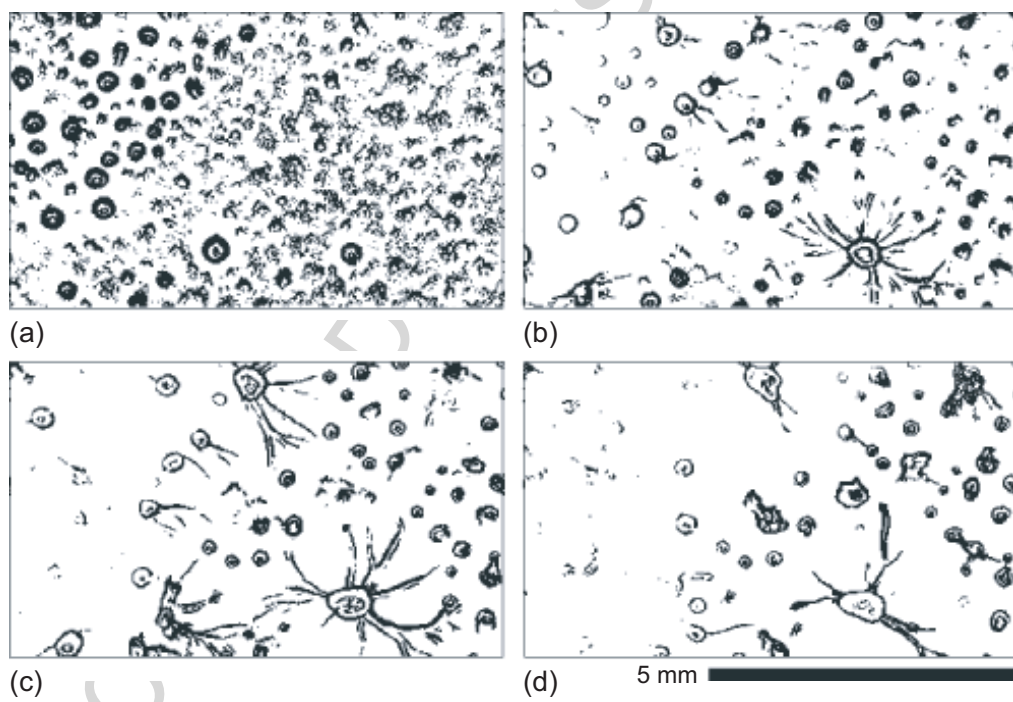


Figure 2:

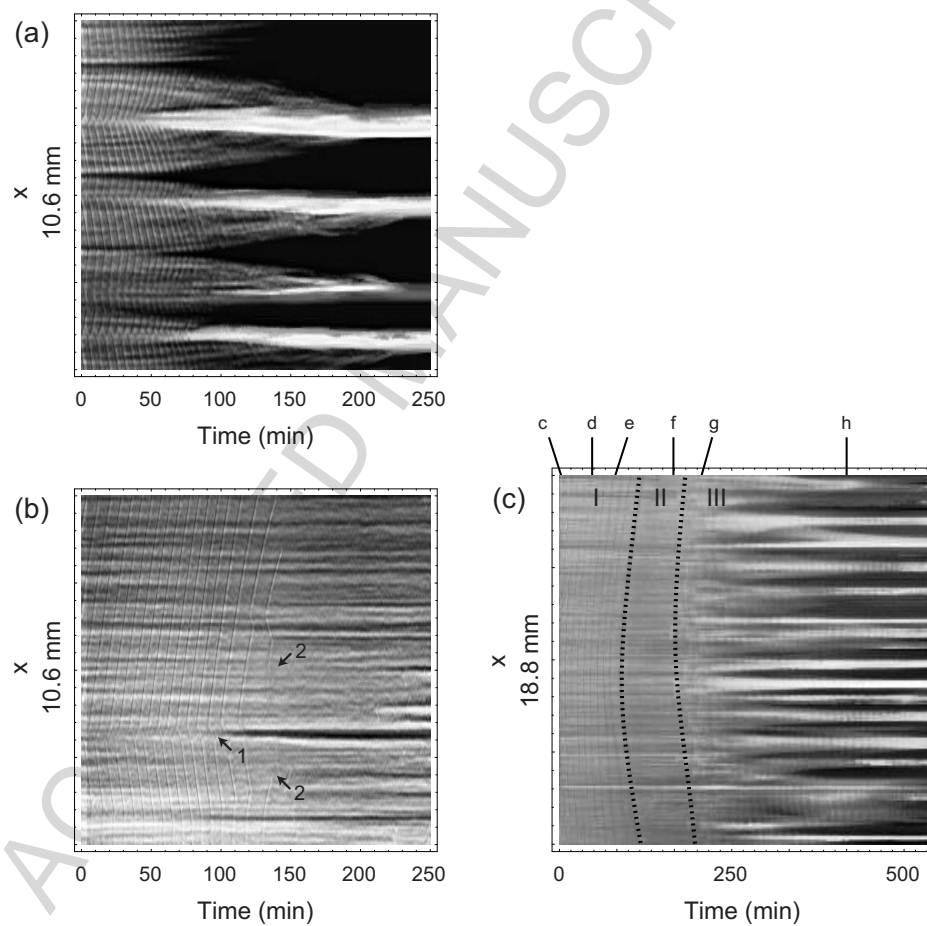


Figure 3:

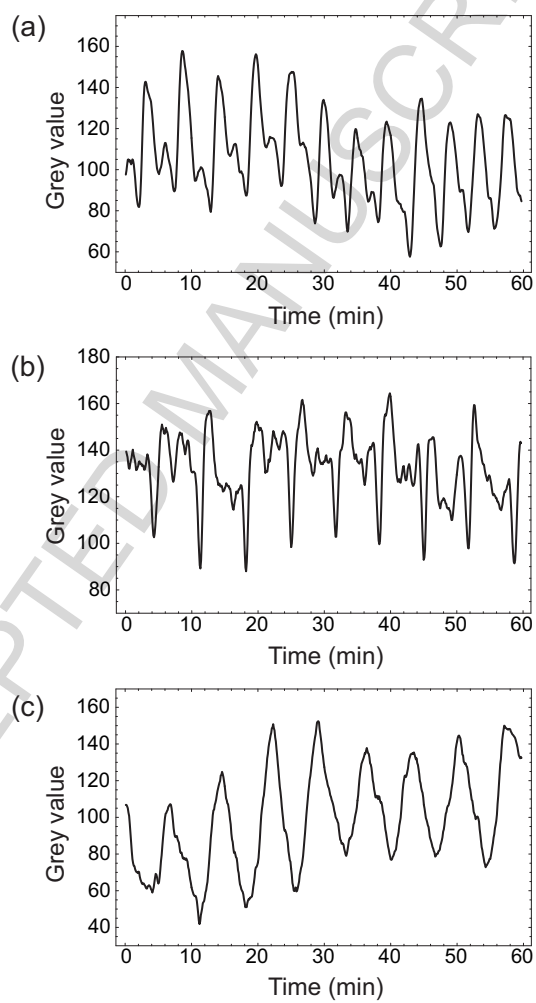


Figure 4:

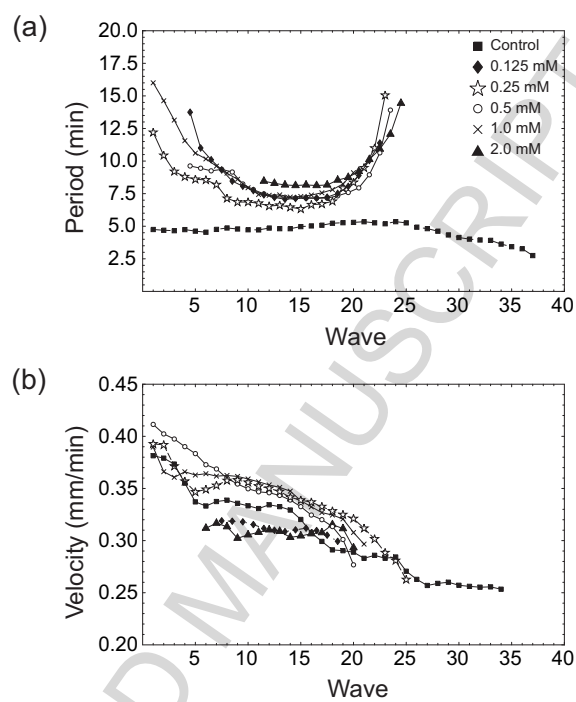


Figure 5:

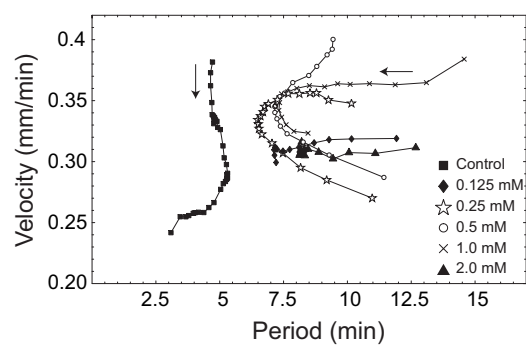


Figure 6:

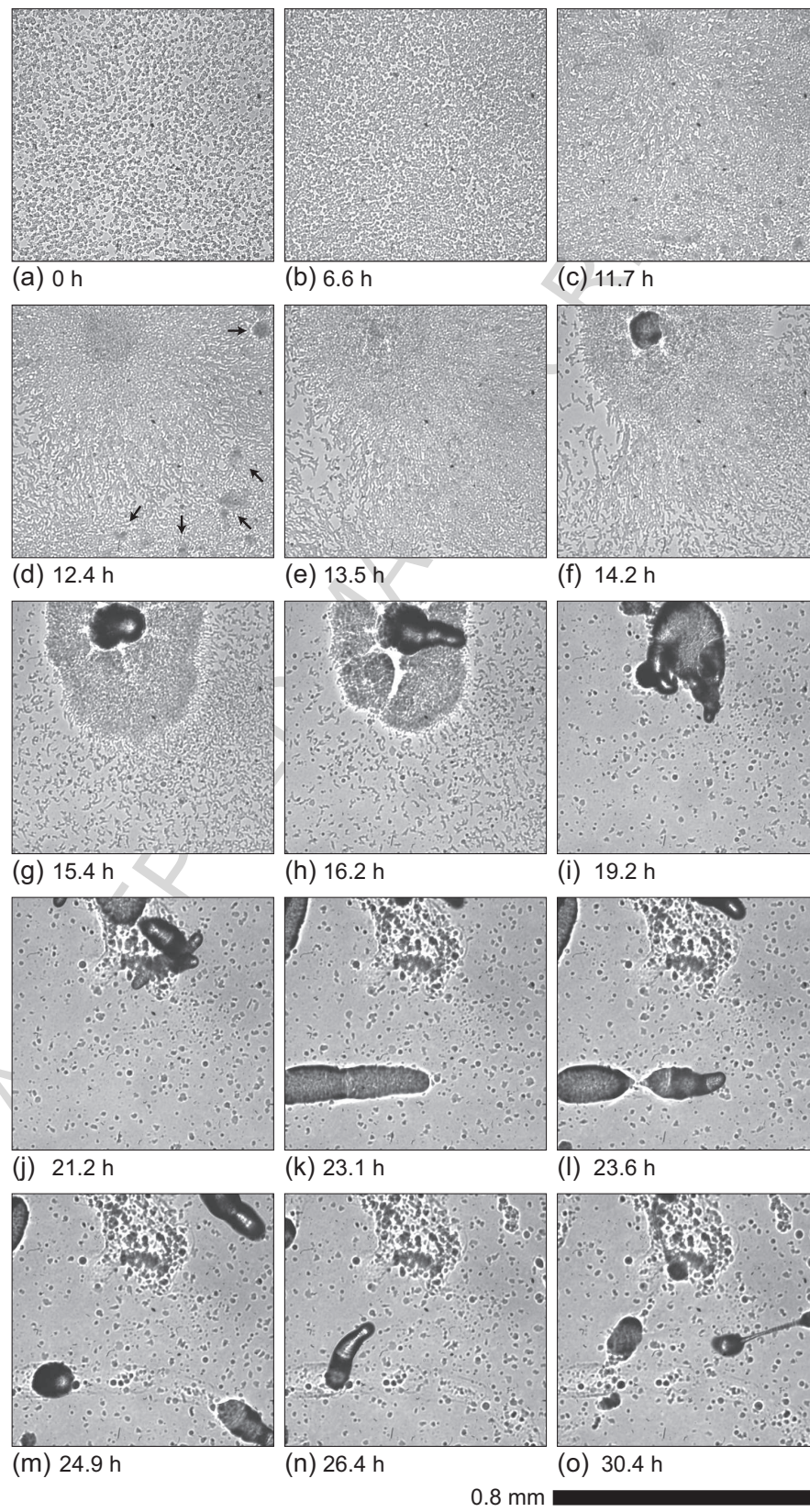


Figure 7:

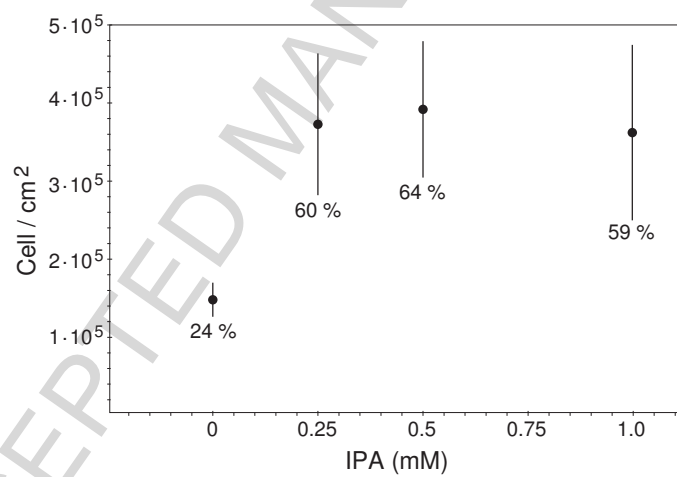


Figure 8: